

Supporting information for:

Cyano substituted benzothiadiazole: a novel acceptor inducing n-type behaviour in conjugated polymers

List of Figures

Figure S1: Optimised geometries of a) DTDCNBT, where a T-DCNBT dihedral angle of 30.12° is predicted and b) DTDFBT where the T-DFBT angle is near planar. A B3LYP level of theory was used with a basis set of 6-31G(d).

Figure S2: HOMO and LUMO electron density plots and optimized geometries of (a) P(Ge-DTDFBT), and (b) P(Ge-DTDCNBT) B3LYP level of theory, basis set of 6-31G(d).

Figure S3: HOMO and LUMO electron density plots and optimized geometries of (a) P(IDT-DTDCNBT) and (b) P(IDT-DTDFBT) B3LYP level of theory, basis set of 6-31G(d).

Table S1: Theoretical HOMO and LUMO levels and band gap calculated using B3LYP level of theory, basis set of 6-31G(d).

Table S2: Device parameters

Figure S4: The crystal structure of DTDCNBT (50% probability ellipsoids).

Figure S5: Transfer (left) and output (right) characteristics for P(Ge-DTDCNBT) in TG/BC configuration under negative gate voltages (untreated Au source/drain electrodes). Hole transport current was so low that the mobility was not calculable.

Figure S6: Transfer (left) and output (right) characteristics for P(Ge-DTDFBT) in TG/BC device configuration with PFBT treated Au source/drain electrodes.

Figure S7: Transfer (left) and output (right) characteristics for P(IDT-DTDCNBT) in BG/TC device configuration.

Figure S8: Transfer (left) and output (right) characteristics for P(IDT-DTDFBT) in BG/TC device configuration.

Figure S9: ^1H NMR spectrum of monomer **3**

Figure S10: ^1H NMR spectrum of P(Ge-DTDCNBT)

Figure S11: ^1H NMR spectrum of P(IDT-DTCNBT)

Figure S12: ^1H NMR spectrum of P(Ge-DTDFBT)

Figure S13: DSC heating and cooling traces of P(IDT-DTDFBT), P(IDT-DTDCNBT), P(Ge-DTDFBT), P(Ge-DTDCNBT) at $20^\circ\text{C}/\text{min}$.

Figure S14: Absorbance spectroscopy of monomer **3** (DTDCNBT) and monomer **4** (DTDFBT) in DCM solution (λ_{max} **3** = 473 nm; λ_{max} **4** 440nm).

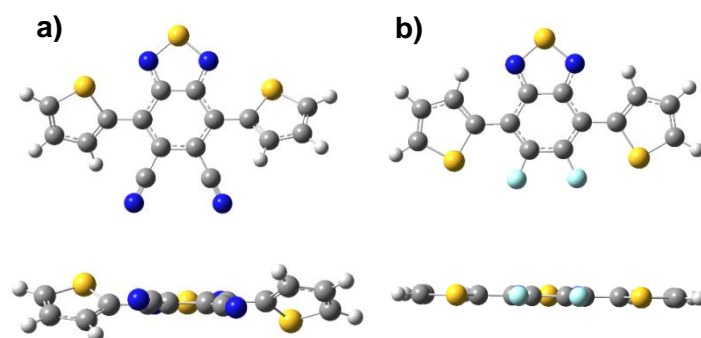


Figure S1: Optimised geometries of a) DTDCNBT, where a T-DCNBT dihedral angle of 30.12° is predicted and b) DTDFBT where the T-DFBT angle is near planar. A B3LYP level of theory was used with a basis set of 6-31G(d).

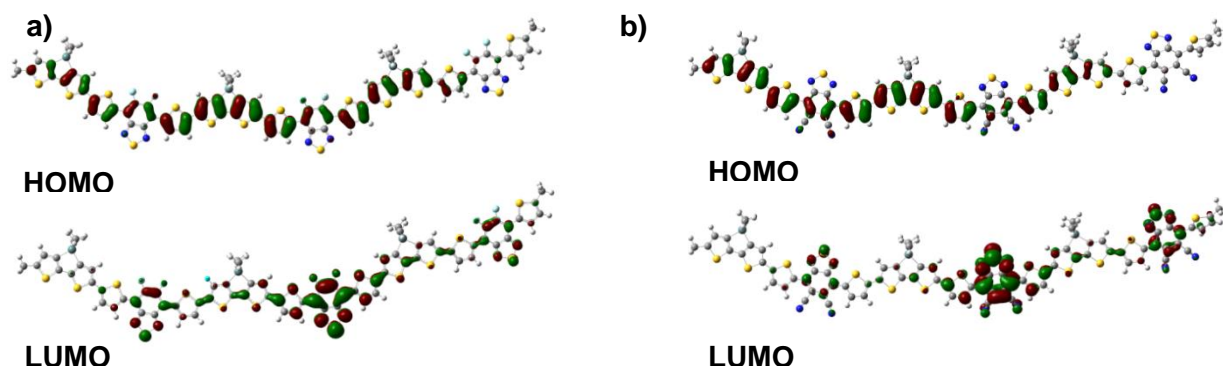


Figure S2: HOMO and LUMO electron density plots and optimized geometries of (a) P(Ge-DTDFBT), and (b) P(Ge-DTDCNBT) B3LYP level of theory, basis set of 6-31G(d).

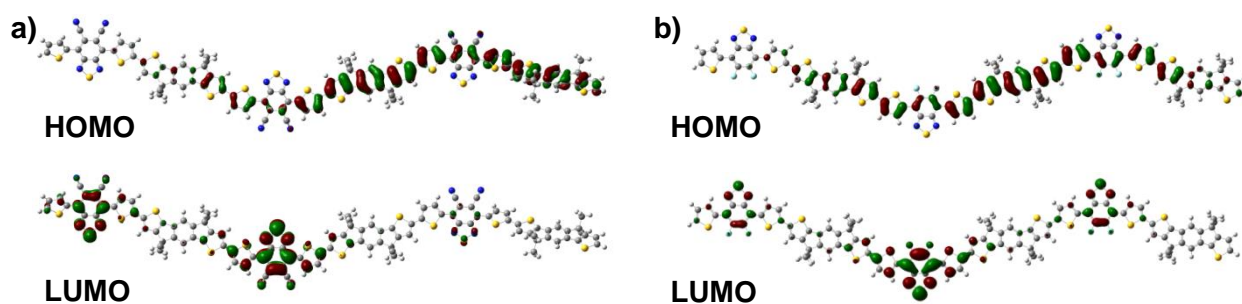


Figure S3: HOMO and LUMO electron density plots and optimized geometries of (a) P(IDT-DTDCNBT) and (b) P(IDT-DTDFBT) B3LYP level of theory, basis set of 6-31G(d).

Table S1: Theoretical HOMO and LUMO levels and band gap calculated using B3LYP level of theory, basis set of 6-31G(d).

Polymer	HOMO	LUMO	E _g
P(Ge-DTDCNBT)	-4.97	-3.72	1.24
P(Ge-DTDFBT)	-4.63	-3.16	1.47
P(IDT-DTDCNBT)	-4.92	-3.66	1.26
P(IDT-DTDFBT)	-4.63	-3.12	1.51

Table S2: Device parameters

Polymer	Device configuration	μ_{lin} (cm ² V ⁻¹ s ⁻¹)	μ_{sat} (cm ² V ⁻¹ s ⁻¹)	V _{Th} (V)	I _{on} /I _{off}
		hole/electron	hole/electron	hole/electron	hole/electron
P(Ge-DTDCNBT)	TG/BC (Au)	na/2.0×10 ⁻³	na/2.8×10 ⁻³	na/43	na/10 ² -10 ³
P(Ge-DTDFBT)	TG/BC (Au-PFBT)	3.2×10 ⁻² /na	6.2 × 10 ⁻² /na	-29/na	10 ³ -10 ⁴ /na
P(IDT-DTDCNBT)	BG/TC (Al/Au)	na/1.4×10 ⁻⁴	na/4.9×10 ⁻⁴	na/38	na/10 ² -10 ³
P(IDT-DTDFBT)	BG/TC (Al/Au)	2.5×10 ⁻² /na	6.1×10 ⁻² /na	-19/na	10 ⁴ -10 ⁵ /na

The X-ray crystal structure of DTDCNBT

Crystal data for DTDCNBT: C₁₆H₆N₄S₃, *M* = 350.43, monoclinic, P2₁/n (no. 14), *a* = 7.1953(4), *b* = 17.8923(9), *c* = 11.5414(5) Å, β = 103.832(5)°, *V* = 1442.76(12) Å³, *Z* = 4, *D*_c = 1.613 g cm⁻³, μ(Mo-Kα) = 0.516 mm⁻¹, *T* = 173 K, orange blocks, Agilent Xcalibur 3E diffractometer; 2870 independent measured reflections (*R*_{int} = 0.0215), *F*² refinement,^[1] *R*₁(obs) = 0.0387, *wR*₂(all) = 0.0885, 2360 independent observed absorption-corrected reflections [*|F_o|* > 4σ(*|F_o|*), 2θ_{max} = 56°], 251 parameters. CCDC 1020253.

Both the C10- and C17-based thiophene rings in the structure of DTDCNBT were found to be disordered. In each case two orientations were identified, of ca. 88:12 and 86:14% occupancy for the C10- and C17-based rings respectively. The geometries of all four rings were optimised, the thermal parameters of adjacent atoms were restrained to be similar, and only the non-hydrogen atoms of the major occupancy orientations were refined anisotropically (those of the minor occupancy orientations were refined isotropically). In each case, the disorder amounts to a swapping of the sulphur position between the two α sites.

[1] SHELXTL, Bruker AXS, Madison, WI; SHELX-97, G.M. Sheldrick, *Acta Cryst.*, 2008, *A64*, 112-122; SHELX-2013, <http://shelx.uni-ac.gwdg.de/SHELX/index.php>

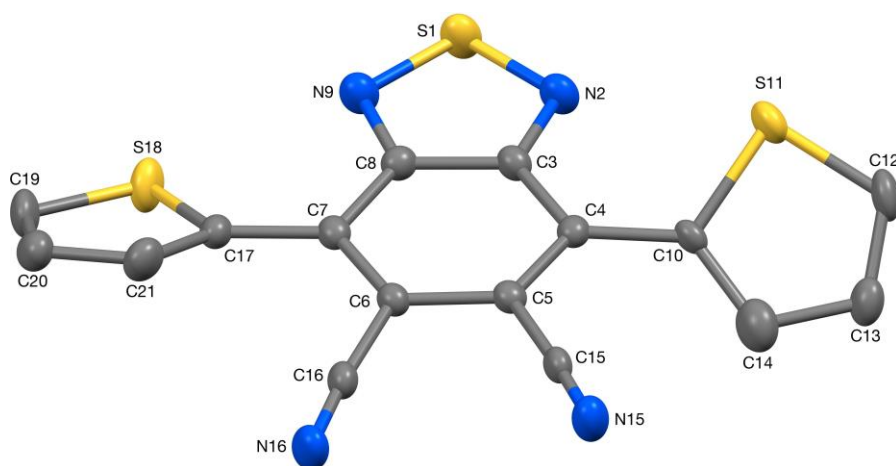


Figure S4: The crystal structure of DTDCNBT (50% probability ellipsoids).

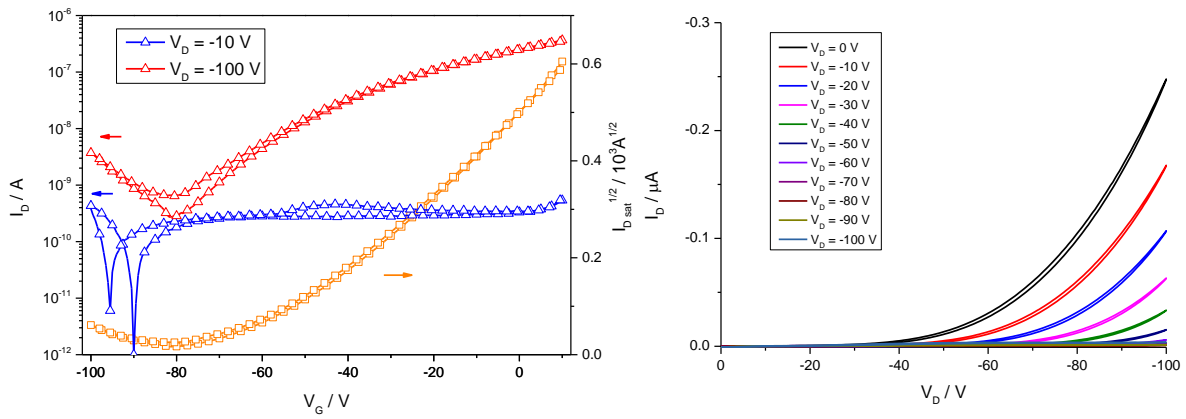


Figure S5: Transfer (left) and output (right) characteristics for P(Ge-DTDCNBT) in TG/BC configuration under negative gate voltages (untreated Au source/drain electrodes). Hole transport current was so low that the mobility was not calculable.

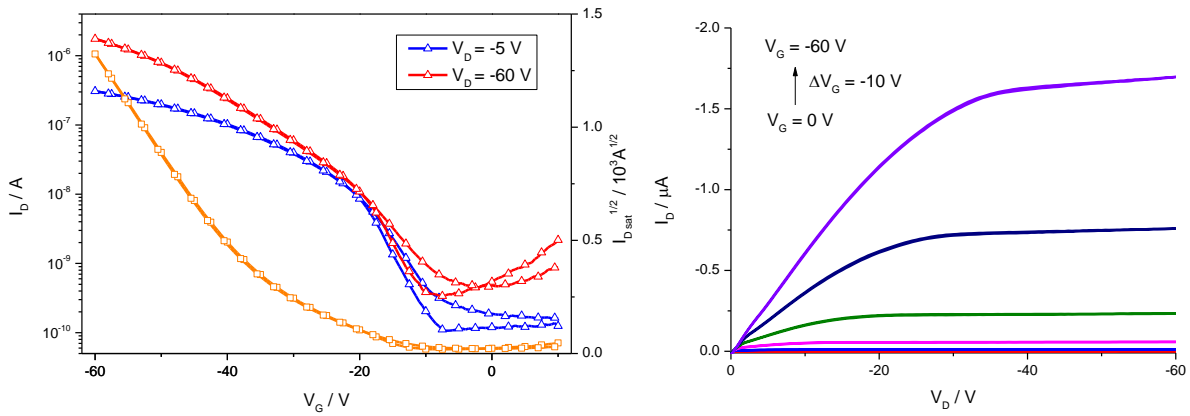


Figure S6: Transfer (left) and output (right) characteristics for P(Ge-DTDFBT) in TG/BC device configuration with PFBT treated Au source/drain electrodes.

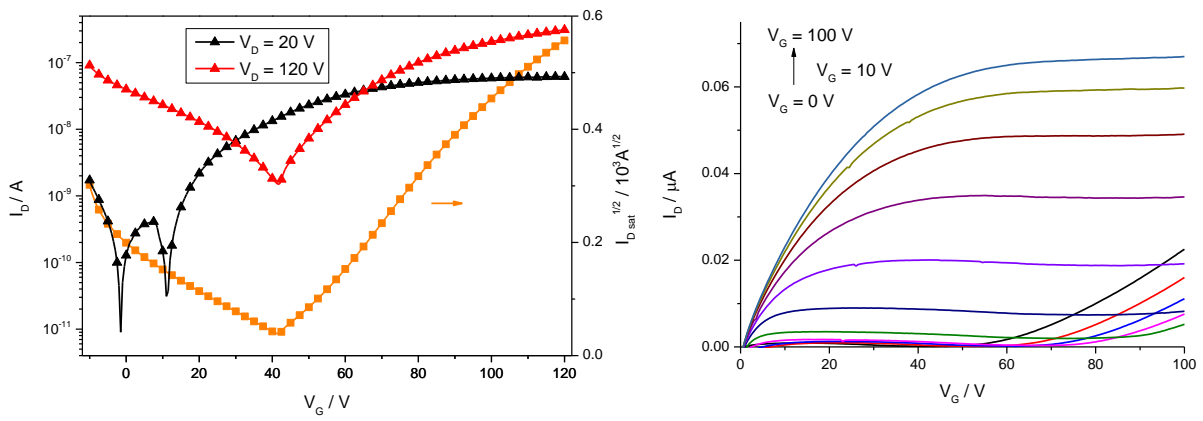


Figure S7: Transfer (left) and output (right) characteristics for P(IDT-DTDCNBT) in BG/TC device configuration.

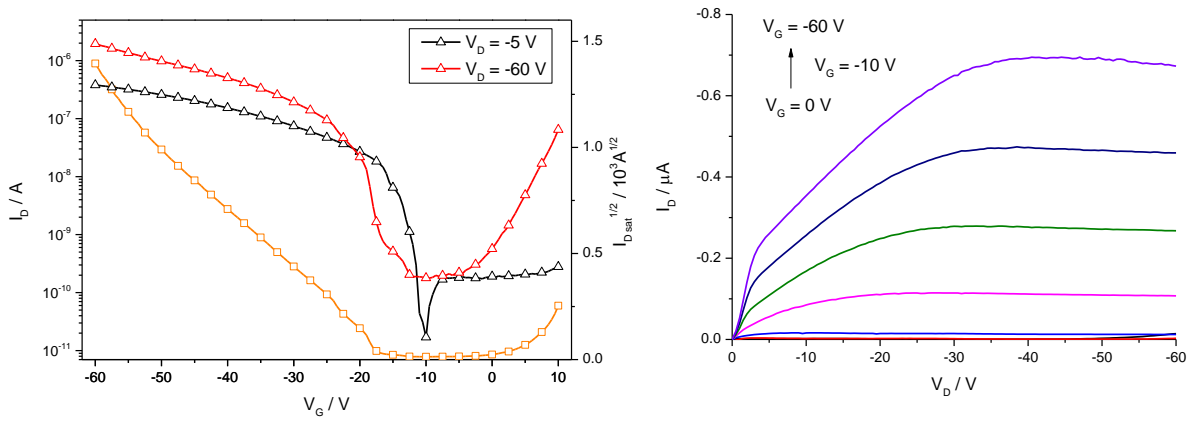


Figure S8: Transfer (left) and output (right) characteristics for P(IDT-DTDFBT) in BG/TC device configuration.

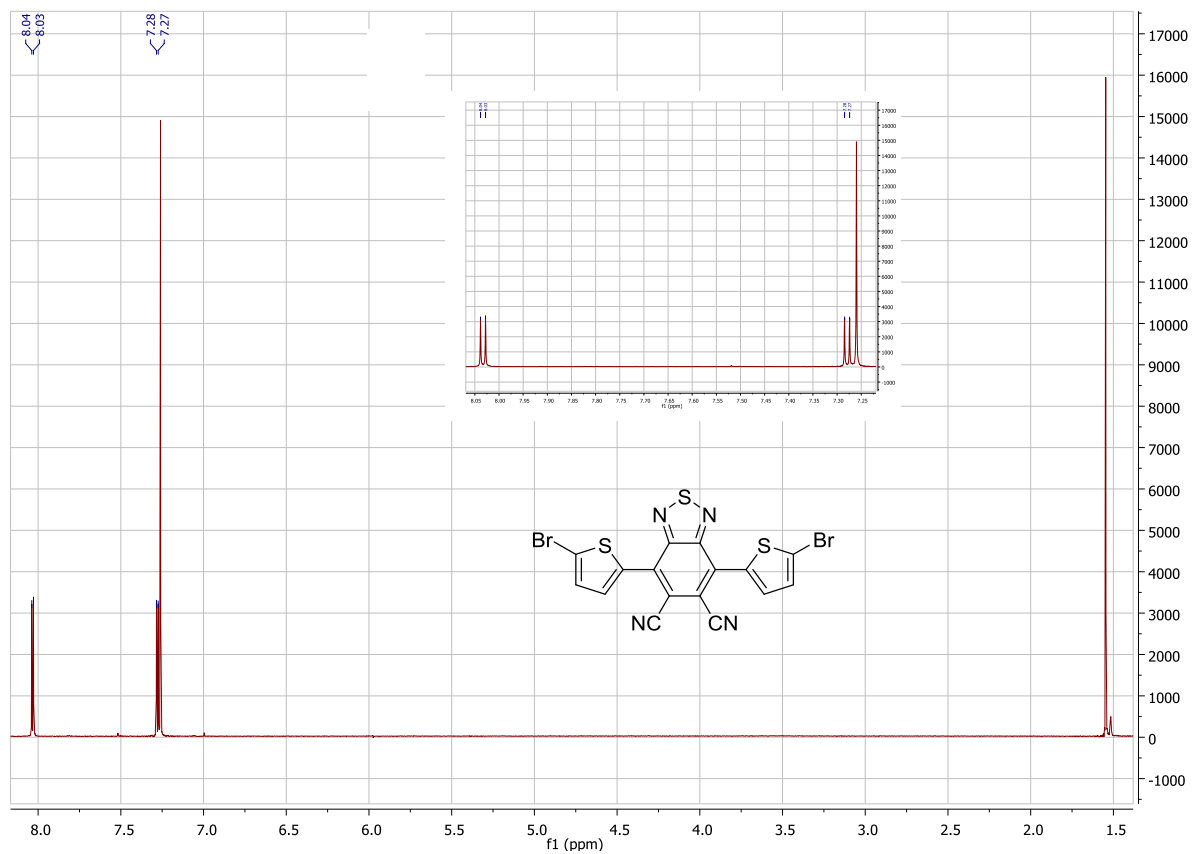


Figure S9: ^1H NMR spectrum of monomer **3**

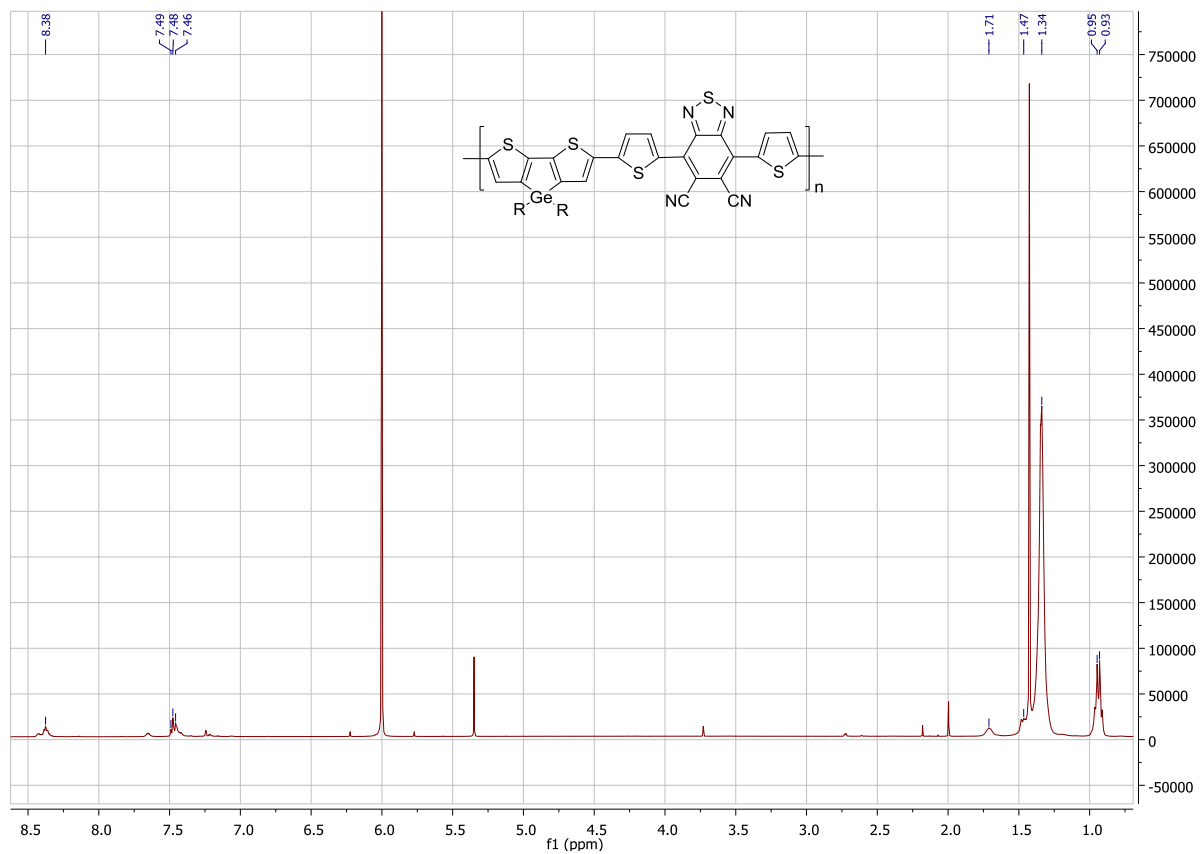


Figure S10: ^1H NMR spectrum of P(Ge-DTDCNBT)

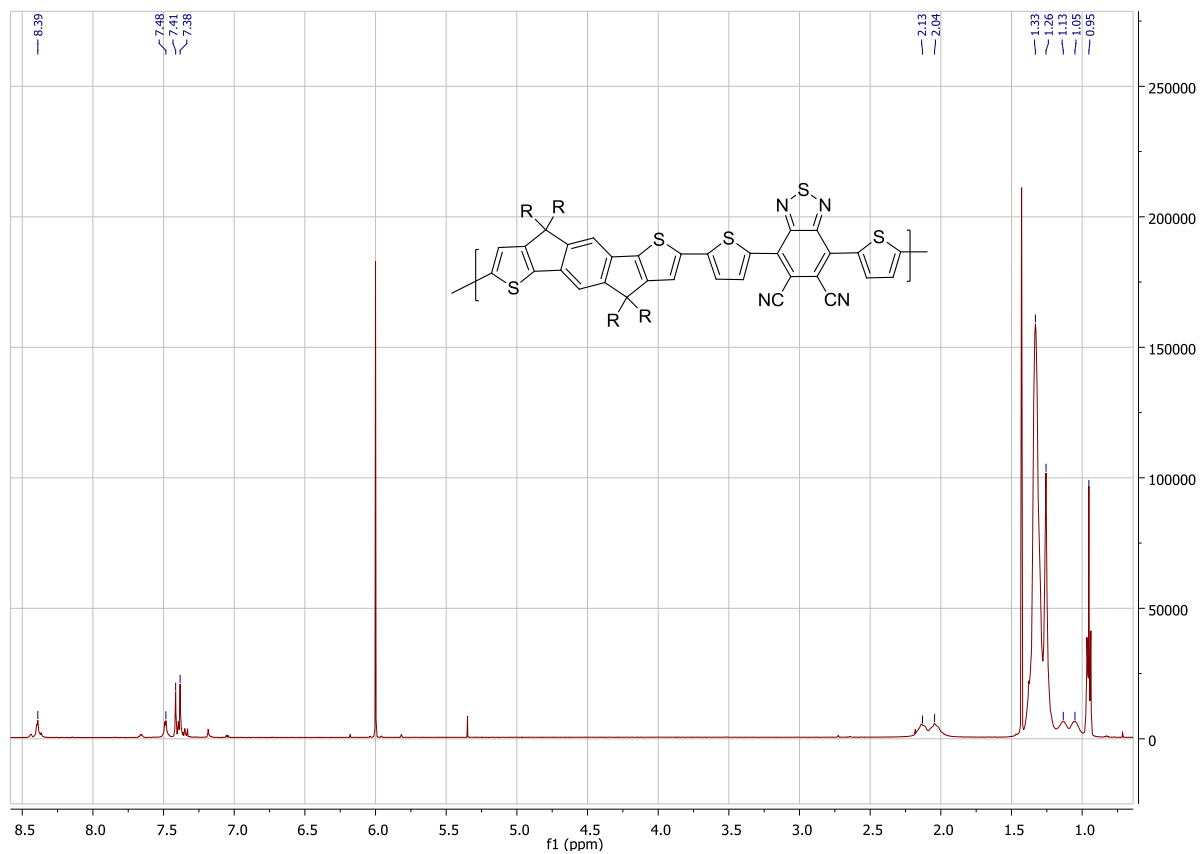


Figure S11: ¹H NMR spectrum of P(IDT-DTCNBT)

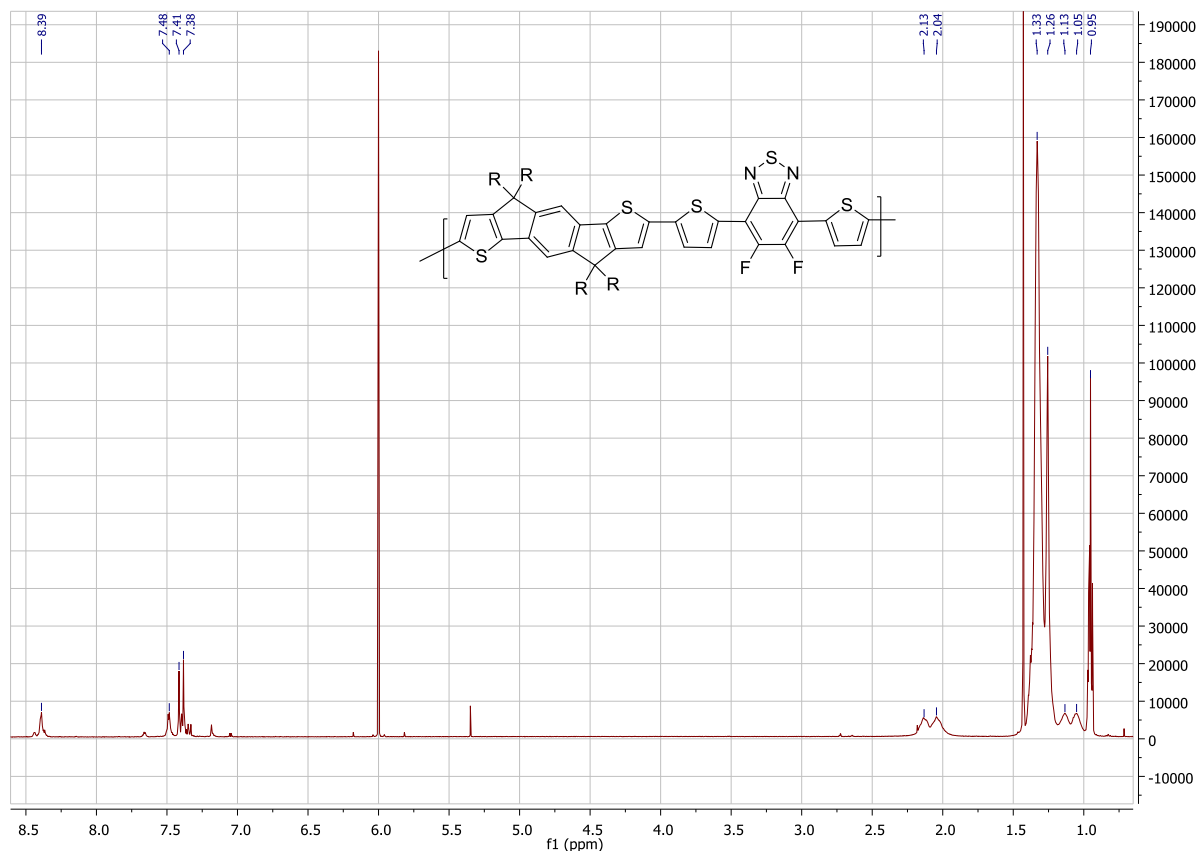


Figure S12: ^1H NMR spectrum of P(Ge-DTDFBT)

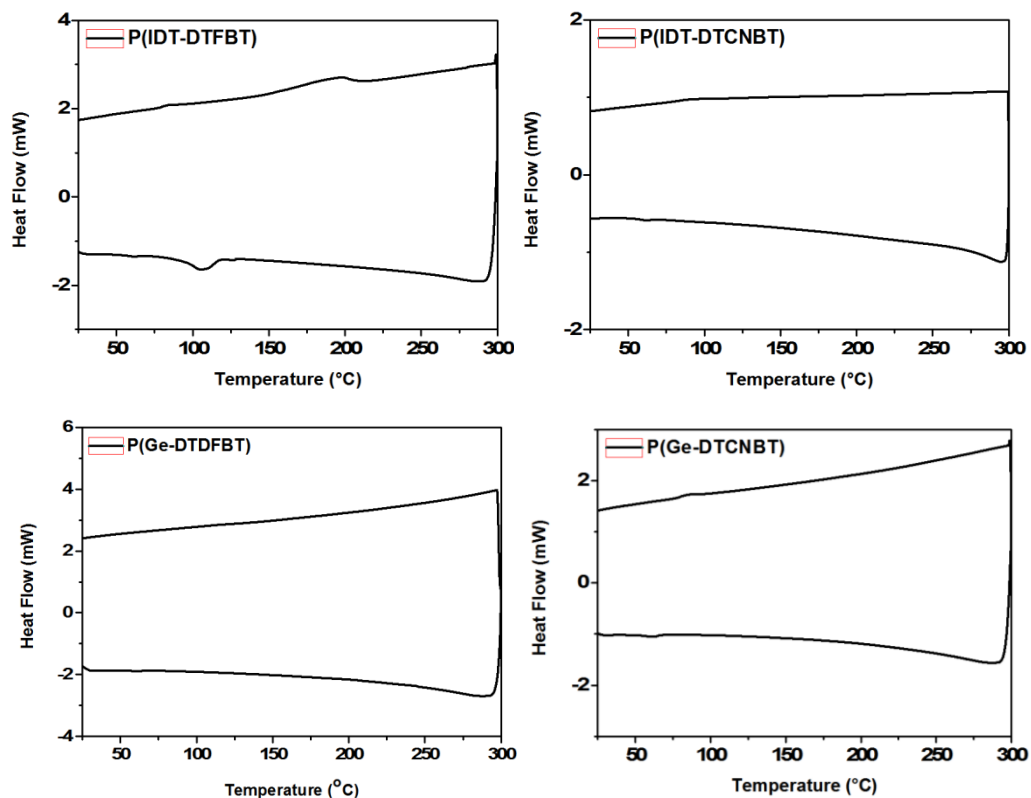


Figure S13: DSC heating and cooling traces of P(IDT-DTDFBT), P(IDT-DTDCNBT), P(Ge-DTDFBT), P(Ge-DTDCNBT) at 20°C/min.

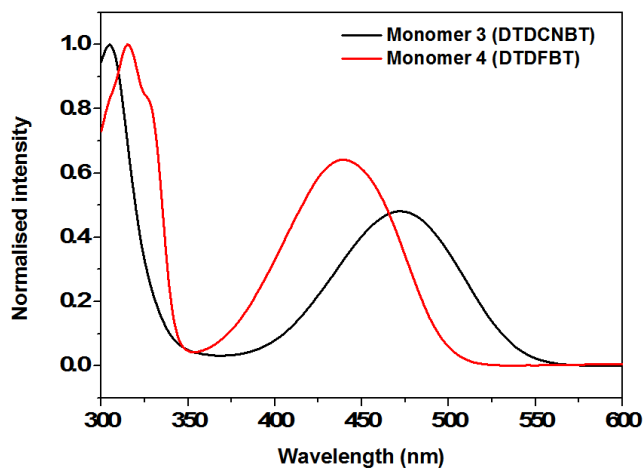


Figure S14: Absorbance spectroscopy of monomer **3** (DTDCNBT) and monomer **4** (DTDFBT) in DCM solution (λ_{\max} **3** = 473 nm; λ_{\max} **4** 440nm).